Mechanical Signals Activate Vascular Endothelial Growth Factor Receptor-2 To Upregulate Endothelial Cell Proliferation during Inflammation

Jie Liu and **Sudha Agarwal**

Biomechanics and Tissue Engineering Laboratory, Division of Oral Biology, The Ohio State University College of Dentistry, Columbus, OH 43210

Abstract

Signals generated by the dynamic mechanical strain critically regulate endothelial cell proliferation and angiogenesis; however, the molecular basis remains unclear. We investigated the mechanisms by which human dermal microvascular endothelial cells (HDMECs) perceive mechanical signals and relay them intracellularly to regulate gene expression and endothelial cell proliferation. HDMECs were exposed to low/physiologic levels of dynamic strain and probed for the differential activation/inhibition of kinases in the mechanosignaling cascade associated with endothelial cell gene activation. Because angiogenesis is important at inflammatory sites, we also assessed the mechanisms of mechanosignaling in the presence of a proinflammatory cytokine IL-1β. In this article, we demonstrate that the mechanosignaling cascade is initiated by vascular endothelial growth receptor-2 (VEGFR2) activation. Mechanoactivation of VEGFR2 results in its nuclear translocation and elevation of PI3K-dependent Ser473-Akt phosphorylation. Subsequently, activated Akt inactivates the kinase activity of the serine/threonine kinase, glycogen synthase kinase-3β (GSK3β), via its Ser9 phosphorylation. Thus, inactive GSK3β fails to phosphorylate cyclin D1 and prevents its proteosomal degradation and, consequently, promotes endothelial cell survival and proliferation. In the presence of IL-1β, cyclin D1 is phosphorylated and degraded, leading to inhibition of cell proliferation. However, mechanical signals repress cyclin D1 phosphorylation and upregulate cell proliferation, despite the presence of IL-1β. The data indicate that the VEGFR2/Akt/GSK3β signaling cascade plays a critical role in sensing and phosphorelaying mechanical stimuli in endothelial cells. Furthermore, mechanical forces control highly interconnected networks of proinflammatory and Akt signaling cascades to upregulate endothelial cell proliferation.

Biomechanical signals play a critical role in vascular tissue homeostasis, differentiation, pathophysiology, and repair (1, 2). Endothelial cells are constantly exposed to hemodynamic forces in the form of cyclic tensile (stretch) and fluid shear forces as a result of the pulsatile nature of blood pressure and flow (1, 3–5). These cells are equipped to perceive mechanical signals and convert them into biochemical events that affect cell proliferation, migration, and apoptosis, as well as gene expression (6–11). Mechanical forces interact with endothelial cells via extracellular matrix and activate multiple transmembrane molecules, such as integrins, vascular endothelial (VE)-cadherins, TRVP4 ion channel, and caveolae (8, 11–15). Activation of these molecules and focal adhesion complexes on the cell surface

Address correspondence and reprint requests to Dr. Sudha Agarwal, Biomechanics and Tissue Engineering Laboratory, 4010 Postle Hall, 305 West 12th Avenue, The Ohio State University, Columbus, OH 43210. Agarwal.61@osu.edu.

Disclosures
The authors have no financial conflicts of interest.

relays mechanical signals to cytoskeletal microfilaments, microtubules, and intermediate filaments that contribute to the changes in cell structure and functional responses (16, 17).

Intracellularly, activation of small GTPase RhoA and Rac1 kinase by mechanical signals induces endothelial cell proliferation and actin rearrangements. The expression of vascular endothelial cell growth factor receptor-2 (VEGFR2), essential for endothelial cell proliferation and angiogenesis, is controlled by p190RhoGAP, an upstream inhibitor of Rho. Mechanical signals activate p190Rho-GAP by balancing the binding of transcription factors TFII-I and GATA2 to the VEGFR2 promoter region and regulate its expression (1, 8, 18). Activation of MAPKs was shown to be associated with pressure-induced heparan sulfate glycosaminoglycans synthesis (19). Nevertheless, the mechanisms by which endothelial cells integrate biophysical signals and transduce them in the cytoplasmic domain of cells to regulate gene expression and neovascularization in healthy or inflamed tissues remains to be explained.

Vascular endothelial growth factor (VEGF) and its receptors are essential for normal angiogenesis and sequentially activate pathways that lead to endothelial cell proliferation, migration, and eventual capillary tube formation (20). This is also evident by the fact that VEGFR2 deregulation leads to tissue pathologies (21). Interestingly, shear stress leads to the induction of VEGFR2 in endothelial cells (1, 22–24). Serine/threonine protein kinase B/Akt signaling is a critical regulator of endothelial cell survival and proliferation. Upon receptor activation, Akt is recruited to the plasma membrane, binds to the lipid PI3K products, and is activated by phosphorylation at Thr308 and Ser473 residues. Activated Akt, in turn, phosphorylates and inactivates a serine/threonine kinase, glycogen synthase kinase-3β (GSK3β), at Ser9 (25). GSK3β is a proapoptotic kinase implicated in the regulation of cell fate. Over-expression of active GSK3β can cause cell-cycle arrest. GSK3β phosphorylates cyclin D1 at Thr286, thereby triggering its proteasomal degradation and cell-cycle arrest (26, 27). Phosphorylation and inactivation of GSK3β by Akt stabilizes cyclin D1 and results in the prolongation of cyclin D1 half-life and, hence, upregulation of the cell-cycle progression, essential for angiogenesis (28, 29).

During inflammation, proinflammatory cytokines and elaborated mediators, such as reactive oxygen species and matrix metalloproteinases, as well as recruited immune cells, create an environment geared toward tissue destruction and disorganization. IL-1β and TNF-α act as potent initiators, mediators, and perpetuators of inflammation. Elaboration of IL-1β by inflammatory cells can induce apoptosis and suppress proliferation of endothelial cells (30–32). Furthermore, addition of IL-1R antagonist to block IL-1 signaling by binding to IL-1R1 increases proliferation and the life span of endothelial cells (33). IL-1 also transforms human dermal microvascular endothelial cells (HDMECs) to myofibroblasts, which may reduce vascularity and upregulate fibrosis in wounds (34). Thus, in such an antiangiogenic environment, tissue repair must largely be facilitated by the ability of endothelial cells to continuously evade actions of destructive mediators and create new capillaries to reconstruct the tissue lost to inflammatory processes (35). Based on these observations, we further investigated whether mechanical signals play a role in supporting angiogenesis in an inflammatory environment. In this article, we show that these signals abrogate the actions of inflammatory cytokines and support activation of VEGFR2-dependent signaling pathways, allowing endothelial cell proliferation in an inflammatory environment.

Materials and Methods

Cell culture

HDMECs were purchased (Cell Applications, San Diego, CA) and cultured in VascuLife VEGF-Mv Medium (Lifeline Cell Technology, Walkersville, MD), supplemented with

penicillin (100 U/ml) and streptomycin (100 µg/ ml). These cells were further characterized for the presence of von Willebrand factor and CD31. HDMECs were used at passages 3–5, during which the cell morphology, growth rate, and phenotypic characteristics remain stable.

Application of cyclic strain

HDMECs (8×10^4/well) were seeded on collagen I-coated BioFlex six-well culture plates (Flexcell International, Hillsborough, NC) and grown in VascuLife VEGF-Mv Medium to 80% confluence in 5% CO_2 and 37°C (3–4 d). Eighteen hours prior to experimentation, the medium was replaced by MCDB 131 medium (Caisson Laboratories, Logan, UT) supplemented with 1% FBS (Atlanta Biologicals, Norcross, GA), penicillin (100 U/ml), streptomycin (100 µg/ml), and 2 mM L-glutamine (Invitrogen, Carlsbad, CA) for serum and growth factor starvation. Cells were subsequently subjected to Dynamic Tensile Strain (DTS) of various magnitudes (3, 6, and 12%) and frequencies (0.25, 0.1, and 0.05 Hz) using a Flexcell 4000T/FlexLink Cell Culture System (Flexcell International). HDMECs were exposed to four treatment regimens: untreated controls, cells treated with recombinant human IL-1β alone (2 ng/ml; Calbiochem, San Diego, CA), cells treated with DTS alone, and cells treated with DTS and recombinant human IL-1β together to examine the effects of DTS under proinflammatory conditions. For inhibitor studies, HDMECs were preincubated for 1 h with 1 or 10 µM selective VEGFR2 inhibitor SU5416 (Calbiochem) or 10 or 50 µM PI3K inhibitor LY294002 (Cayman Chemical, Ann Arbor, MI) prior to initiation of the experiment.

RNA purification and real-time PCR

As described earlier (36), total RNA was isolated with an RNeasy Mini kit (Qiagen, Valencia, CA), and the concentration, purity, and integrity were assessed by a NanoDrop ND-1000 spectrophotometer. A total of 1 µg RNA was reverse transcribed with 1× First-Strand Synthesis Buffer containing 25 ng/µl oligonucleotide (dT)$_{12–18}$, 3.75 µM random hexamer for 5 min at 65°C. After cooling on ice for 1 min, 1× First-Strand Synthesis Buffer, 5 mM DTT, 10 U/µl Superscript III reverse transcriptase, 2 U/µl RNaseOUT inhibitor (Invitrogen), and 500 µM each deoxynucleotide tri-phosphate (dATP, dTTP, dGTP, and dCTP) were added, and the mixture was incubated at 25°C for 5 min, 55°C for 60 min, and 70°C for 15 min. Real-time PCR was performed in a final volume of 25 µl (Bio-Rad iCycler) iQ SYBR Green Supermix (Bio-Rad, Hercules, CA). The amount of the experimental target was normalized to a housekeeping gene transcript (*Rps18*), relative to a calibrator (untreated control sample or IL-1β–treated sample), and was given as the estimation $2^{-\Delta\Delta CT}$, where $\Delta\Delta C_T = \Delta C_T$(sample) − ΔC_T(calibrator) and ΔC_T is the C_T of the target gene subtracted from the C_T of *Rps18*. Primers used were *Vegfr2* (forward 5′-TGGGAACCGGAACCTCACTATC-3′, reverse 5′-GTCTTTTCCTGGG-CACCTTCTATT-3′), *IL-1β* (forward 5′-GTACCTGAGCTC GCCAGTG-AAA-3′, reverse 5′-GGTCGGAGATTCGTAGCTGGAT-3′), *Tnf-α* (forward 5′-ATGAGCACTGAAAGCATGATCC, reverse 5′-GAGGGCTGATTAGAG-AGAGGTC-3′) and *Rps18* (forward 5′-GGCCGAAGATATGCTCATGTG-GTGT-3′, reverse 5′-GGCCAGTGGTCTTGGTGTGCTG-3′).

Western blot analysis

As described earlier (37), whole-cell proteins were extracted in Ripa buffer (80 µl) containing proteinase inhibitor (Roche Diagnostic, Branchburg, NJ) and phosphatase inhibitor mixture 2 (Sigma-Aldrich, St. Louis, MO). Alternatively, nuclear and cytoplasmic proteins were extracted separately with NE-PER Nuclear and Cytoplasmic Extraction Reagents (Pierce, Rockford, IL). Protein concentration was determined with bicin-choninic acid protein assay reagents (Pierce) and estimated by a Victor 1420 Multilabel Counter (PerkinElmer, Boston, MA). Lysates normalized for total protein were resolved on

SDS-10% PAGE and electrophoretically transferred onto a nitrocellulose membrane (Bio-Rad), blocked in 5% non-fat milk, and probed with anti-VEGFR2, anti–phospho-Tyr1175-VEGFR2, anti–total-Akt, anti–phospho-Ser473-Akt, anti–phospho-Ser9-GSK3β, anti–phospho-Thr286-cyclinD1, anti-cyclinD1 (Cell Signaling Technology, Beverley, MA), or anti–β-actin (Sigma-Aldrich) at 4°C overnight. Subsequently, blots were washed and incubated in IRDye 680 or IRDye 800 conjugated goat anti-rabbit or goat anti-mouse IgG (LI-COR, Lincoln, NE), washed three times with PBS-0.1% Tween 20, imaged using an ODYSSEY imager (LI-COR), and quantitatively analyzed using ODYS-SEY application software, ver. 2.1.

Immunofluorescence

Following treatments, HDMECs were washed with ice-cold PBS, fixed in 2% paraformaldehyde (pH 8) for 40 min, and permeabilized with 0.2% Triton X-100. Subsequently, the flexible silicone membranes from BioFlex plates were excised and divided into equal pie-shaped pieces. The membranes were blocked with 5% goat serum in blocking buffer (Thermo Shandon, Pittsburgh, PA) and incubated with primary Abs (anti–phospho-Tyr1175-VEGFR2 or anti–phospho-Ser473-Akt) in 0.5% BSA-PBS at 4°C overnight. The membranes were washed with PBS-Tween and then incubated with Cy3-conjugated goat anti-rabbit IgG for 120 min at room temperature. Cells were counterstained with FITC-conjugated phalloidin (Invitrogen) to visualize F-actin. The membranes were mounted with Vectashield Mounting Medium (Vector Laboratories, Burlingame, CA), examined under epifluorescence using a Zeiss Axioplan microscope, and immunofluorescence images were captured with Zeiss Axiovision imaging software.

Cell-proliferation assay

The cell proliferation was examined by the MTT cell-proliferation assay (American Type Culture Collection, Manassas, VA), according to the manufacturer's recommended protocol. HDMECs were grown in VEGF-Mv Medium to reach 50% confluence before treatment with IL-1β/DTS/DTS +IL-1β in 1% FBS 131 medium for 60 min. After treatment, medium was changed back to VEGF-Mv Medium. The same procedures were repeated for 2 d. On day 3, cells were incubated for 3 h with 100 μl/ml MTT. The formazan formation was assessed by absorbance at 570 nm (Victor Plate Reader, PerkinElmer). The cell-proliferation rate was calculated as mean absorbance of treated cells DTS/mean absorbance of controls.

Cell-apoptosis assay

The cell apoptosis was examined using the Annexin V-EGFPApoptosis Detection kit (BioVision, San Francisco, CA). HDMECs were grown on BioFlex plates in VEGF-Mv Medium to reach 50% confluence before treated with IL-1β/DTS/DTS+IL-1β in 1% FBS 131 medium for 60 min. After treatment, medium was changed back to VEGF-Mv Medium. The same procedures were repeated for 2 d. On day 3, HDMECs on the Bioflex plates were washed with ice-cold PBS. Subsequently, a pie-shaped piece of the flexible silicone membrane were excised and incubated for 5 min in the dark with Annexin V-EGFP, according to the kit instructions. Then, the membranes were mounted with ProLong Gold Antifade Reagent with DAPI (Invitrogen) and visualized under epifluorescence using a Zeiss Axioplan microscope; immunofluorescence images were captured with Zeiss Axiovision imaging software. Cells that have bound Annexin V-EGFP (apoptotic cells) showed green staining in the plasma membrane.

Statistical analysis

Results are expressed as the mean ± SE from three independent experiments. Statistical analysis was performed using one-way ANOVA and a post hoc Tukey test using Minitab 14 Statistical Software. Results were considered statistically significant when $p < 0.05$.

Results

Mechanical signals activate VEGFR2

VEGFR2 is essential for normal vascular endothelial cell proliferation, migration, and angiogenesis. Therefore, we speculated that induction of angiogenesis by mechanical strain may also require VEGFR2 activation for downstream signaling. In these experiments, HDMECs were exposed to DTS (6%, 0.25 Hz) for various time intervals in the presence or absence of IL-1β, to mimic the tensile forces experienced by HDMECs under physiological conditions and during inflammation. Control cells and cells exposed to IL-1β did not induce VEGFR2 phosphorylation at any time point tested (Fig. 1*A*, 1*B*). In contrast, HDMECs exposed to DTS demonstrated a rapid induction of VEGFR2 phosphorylation, which was observed within 5 min and gradually diminished over a 2-h period. More significantly, VEGFR2 was phosphorylated by DTS in the presence of IL-1β, suggesting that mechanical signals can upregulate VEGFR2-mediated cellular responses in an inflammatory environment (Fig. 1*A*, 1*B*). These effects of DTS are similar to VEGF itself, which is known to activate VEGFR2. Furthermore, we observed that VEGF can also activate VEGFR2 in the presence of IL-1β (data not shown). In these cells, VEGFR1 was also minimally activated, whereas VEGFR3 did not transmit signals induced by mechanical strain (data not shown).

To analyze whether the phosphorylation of VEGFR2 represents a mechanism whereby mechanical signals upregulate VEGFR2 expression, we tracked phospho-VEGFR2 nuclear translocation in HDMECs by immunofluorescence. Phospho-Tyr1175-VEGFR2 translocated to the nucleus within 5 min of mechanoactivation and was found in the nucleus for the ensuing 60 min. Subsequently, its gradual re-expression in the cytoplasmic compartment was paralleled by its reduction in the nucleus during the next 60 min (Fig. 1*C*). To further confirm these findings, we examined the presence of VEGFR2 in the nuclear and cytoplasmic extracts of HDMECs. As shown in Fig. 1*D*, the majority of phosphorylated VEGFR2 was present in the nuclear fraction, with minimal presence in the cytoplasm. Consequently, a 4.94 ± 0.27-fold and 2.16 ± 0.17-fold induction of *Vegfr2* mRNA expression was observed after 2 and 4 h of mechanoactivation, respectively (Fig. 1*E*).

We next investigated whether VEGFR2 activation is a prerequisite for mechanoactivation of HDMECs. In these experiments, cells were exposed to SU5416, an ATP competitive inhibitor of VEGFR2, prior to mechanoactivation, and phosphorylation of Ser473-Akt was assessed by Western blot analysis. The results revealed that signals generated by biomechanical forces were recognized by VEGFR2, because SU5416 inhibited Akt activation by 53.8 and 98% at concentrations of 1 and 10 μM, respectively (Fig. 1*F*). Additionally, 1 and 10 μM SU5416 also markedly downregulated the mechanical signal-induced *Vegfr2* mRNA expression (Fig. 1*G*).

Mechanoactivation of VEGFR2 leads to Akt activation in HDMECs

Because Akt signaling is associated with VEGFR2 activation, we speculated that mechanical forces might activate Akt signaling in HDMECs. The extent of mechanical forces experienced by the cells is markedly influenced by the changes in mechanical integrity of tissue. Therefore, we first investigated the potential consequences of changes in the mechanical environment on the phosphorylation of Ser473 residue on Akt, a site associated with its activation. HDMECs were activated by exposure to DTS of various

magnitudes (0, 3, 6, and 12%), and the phosphorylation of Ser473-Akt was analyzed by Western blot analysis. Under static conditions, HDMECs did not exhibit notable Ser473-Akt phosphorylation. Nevertheless, a marked dose-dependent increase in Akt-Ser473 phosphorylation was observed in response to diverse magnitudes of DTS, which was optimal at 6% and then decreased at 12% DTS (Fig. 2A). As expected, dynamic forces were essential for Akt activation, with a peak at 0.25 Hz (Fig. 2B). In the next series of experiments, exposure of HDMECs to DTS of 6% magnitude at 0.25 Hz revealed that mechanoactivation of HDMECs led to a rapid and sustained activation of Ser473 on Akt, which was observed within 5 min and persisted up to 2 h (Fig. 2C, 2D). Importantly, immunofluorescence analysis revealed that application of cyclic strain for various time intervals induced a rapid and sustained nuclear translocation of phopho-Ser437 Akt to the nucleus between 5 and 60 min. This was followed by a re-expression of phospho-Ser437 Akt in the cytoplasm (Fig. 2E). VEGFR2-dependent Akt activation requires PI3K activity, because pretreatment of cells with LY2940024 abrogated cyclic strain-induced phosphorylation of Akt at Ser473 (Fig. 2F).

At the site of inflammation, angiogenesis prevails in an environment rich in proinflammatory cytokines, such as IL-1β and TNF-α, which induce cytotoxicity and inhibit cell proliferation (38, 39). Because mechanoactivation of HDMECs led to Akt phosphorylation in the above experiments, we investigated whether mechanical signals also play a role in providing proangiogenic signals in a proinflammatory environment to upregulate angiogenesis. To compare the extent of endothelial cell mechanoactivation in the presence of inflammation, HDMECs were subjected to optimal magnitudes of DTS in the presence of IL-1β, and Akt phosphorylation was assessed as a marker of HDMEC activation. Phospho-Ser473-Akt was not observed in control cells and was only seen at minimal levels in cells treated with IL-1β under static conditions (Fig. 2C, 2D). Contrarily, DTS exposure resulted in a significant stimulation of Ser473-Akt phosphorylation at all magnitudes and frequencies tested in the presence and absence of IL-1β.

Mechanoactivation promotes endothelial cell survival via GSK3β phosphorylation

GSK3β, a ubiquitously expressed serine/threonine kinase, is implicated in the regulation of cell fate. In its unphosphorylated state, GSK3β phosphorylates Thr286-cyclin D1 to trigger its ubiquination and subsequent proteolytic degradation to initiate proapoptotic signals and cell-cycle arrest. To evaluate the involvement of GSK3β in mechanoactivation, we next examined its phosphorylation at Ser9, a site associated with its kinase activity. Control cells exhibited minimal GSK3β in the phosphorylated state, which remained low after the addition of IL-1β. Mechanoactivation of HDMECs caused a robust phosphorylation of Ser9-GSK3β within 5 min, which was sustained for the next 30 min and then gradually declined to initial levels by 2 h. Moreover, mechanoactivation induced GSK3β phosphorylation in the presence of IL-1β (Fig. 3A, 3B).

Inactivated GSK3β stabilizes cyclin D1 that is required for the upregulation of the cell-cycle progression essential for angiogenesis. Therefore, to evaluate whether mechanoactivation regulates dephosphorylation of cyclin D1, cells were exposed to DTS in the presence or absence of IL-1β, and the extent of cyclin D1 phosphorylation was examined by Western blot analysis. In unstimulated cells, the majority of cyclin D1 was unphosphorylated, whereas low levels of cyclin D1 were in the phosphorylated state, as a result of its proteosomal degradation. However, HDMECs exposed to IL-1β alone showed a significant upregulation of cyclin D1 phosphorylation within 5 min, which was paralleled by its decrease in the cells during the ensuing 2 h. In contrast, mechanoactivation alone significantly suppressed cyclin D1 phosphorylation to preserve cyclin D1, as evidenced by the increase in total unphosphorylated cyclin D1 in cells (Fig. 3C–E). Additionally, mechanoactivation suppressed the phosphorylation of cyclin D1 induced by IL-1β, which

was paralleled by a significant upregulation of total unphosphorylated cyclin D1 ($p < 0.05$). In these experiments, β-actin was probed to confirm equal protein input in all lanes.

Mechanoactivation induces HDMEC proliferation

Finally, we examined whether cyclin D1 dephosphorylation leads to cell proliferation in HDMECs. Cells were exposed to DTS for 60 min/d for 2 d and analyzed for cell proliferation on day 3 by the addition of MTT; its subsequent reduction revealed that cyclic strain was a robust proliferative signal, inducing a 1.42 ± 0.08-fold increase over control cells ($p < 0.05$). IL-1β suppressed >30% of the HDMEC proliferation. However, despite the presence of IL-1β, a 1.49 ± 0.07-fold increase in cell proliferation induced by DTS was observed compared with cells exposed to IL-1β ($p < 0.05$; Fig. 3*F*).

Examination of cell apoptosis revealed that IL-1β induced a 9.31 ± 2.35-fold increase in apoptotic cells over control cells ($p < 0.05$), whereas DTS suppressed IL-1β–induced cell apoptosis up to 4.03 ± 0.64-fold over control (Fig. 3*F*).

Mechanical signals suppress IL-1β–induced proinflammatory gene induction

In HDMECs, mechanical signals suppressed IL-1β–induced inhibition of endothelial cell proliferation. Hence, to determine the effects of mechanoactivation of HDMECs in IL-1β–induced inflammation, IL-1β–induced *IL-1β* and *Tnf-α* induction was determined. As shown in Fig. 3*G* and 3*H*, control untreated cells did not exhibit *IL-1β* or *Tnf-α* mRNA expression. Similarly, mechanoactivation alone did not induce *IL-1β* or *Tnf-α* mRNA expression. However, as expected, IL-1β induced a dramatic increase in *IL-1β* and *Tnf-α* mRNA expression after 2 and 4 h of treatment. Interestingly, HDMECs exposed to IL-1β and DTS simultaneously exhibited a >95% reduction in mRNA expression for *IL-1β* after 2 and 4 h of activation and a 56% reduction in mRNA expression of *Tnf-α* after 2 h (Fig. 3*G*, 3*H*).

Discussion

In this study, we delineated the signaling cascades that underlie the proangiogenic potential of biomechanical signals. Our results demonstrated that mechanical signals induce a rapid and sustained phosphorylation of VEGFR2 on Tyr1175, even in the presence of IL-1β, suggesting a mechanosensory role of VEGFR2 in endothelial cells. VEGFR2 is a transmembrane receptor tyrosine kinase. Upon activation by its ligand (VEGF) binding, VEGFR2 get dimerized, followed by autophosphorylation of tyrosine residues in the cytoplasmic kinase domain and recruitment of downstream molecules for signal transduction (40). The exact mechanisms via which biomechanical signals are sensed by VEGFR2 remain unclear. It is likely that biomechanical signals 1) directly induce conformational changes in the receptor itself and facilitate the binding of the receptor catalytic sites with downstream molecules; 2) may cause dimerization or increase the cross-linking of VEGFR2 with other cell surface receptors, such as integrins, to activate VEGFR2 (1); or 3) may function through the release of cryptic VEGF sequestered in the surrounding extracellular matrix, in view of the fact that VEGF also can induce phosphorylation of VEGFR2.

We observed that VEGFR2 activated by mechanical strain translocates to the nucleus, as well as initiates signaling cascades in the cytoplasmic domain. These observations are intriguing and show that mechanical signals mimic the actions of VEGF. In endothelial cells, VEGF–VEGFR2 complexes are rapidly internalized: VEGFR2 translocates to the nucleus and is degraded in the proteasomes through protein kinase C-dependent phosphorylation of the C-terminal domain to control receptor activity and angiogenesis (41).

We observed a sustained presence of phospho-Tyr1175 VEGFR2 in the nucleus between 5 and 60 min and in the cytoplasm between 60 and 120 min. Nuclear translocation of VEGFR2 is also induced by shear stress (42). Such nuclear translocations are common to many receptor tyrosine kinases, such as epidermal growth factor receptor, fibroblast growth factor receptors, and nerve growth factor receptors (43–46). In the nucleus, these receptors directly modulate gene transcription or supplant/complement activation of transcription factors by canonical signaling cascades (47). In fact, mechanoactivation of VEGFR2 also leads to a marked upregulation of *Vegfr2* gene transcription, which is inhibitable by SU5416. These findings suggest that VEGFR2 activation by mechanical signals controls its own gene expression and further reinforces the regenerative potential of mechanical signals. Mechanical signals can activate VEGF receptors in a ligand-independent manner involving PECAM-1, VE-cadherins, and integrins (48–50), and VEGFR2 nuclear translocation was shown to depend on the expression of VE-cadherin (42, 51). It is possible that VEGFR2 complexes with adherens and both are activated in response to mechanotransduction. Whether these cell adherens only facilitate VEGFR2 intracellular translocation or can actually be internalized with VEGFR2 need further investigation.

Because Akt activation was found to be SU5416 sensitive, it further confirms that mechanical signals activate VEGFR2 to upregulate Ser473-Akt phosphorylation. Furthermore, Akt phosphorylation is also inhibitable by LY294002, indicating that Akt phosphorylation occurs via PI3K activation. Interestingly, TRVP4 calcium channels also activate PI3K activity in response to mechanical stimulation (13). This implies that TRVP4 and VEGF receptors can upregulate PI3K activity in response to mechanical strain. It is not clear whether both of these receptors are activated simultaneously or discretely in response to mechanical strain. Because HDMECs perceive mechanical strain in a dose-dependent manner, it is possible that activation of these cell-surface receptors is also dependent upon the threshold of mechanical strain.

phospho-Akt is found in the cytoplasm and in the nucleus of mechanoactivated endothelial cells. In the nucleus, it regulates transcription factors associated with Akt signaling, such as FOXO, mTOR, and Nur77 (52, 53). In the cytoplasm, Akt signaling cascade regulates cell survival/proliferation and protein synthesis/ degradation (54). We observed minimal phospho-Ser473-Akt and phospho-Ser9-GSK3β levels in control cells. However, following activation by mechanical strain, these levels rapidly increased, with a phospho-Akt peak at 15 min and a phospho-GSK3β peak at 30 min. Phosphorylation of GSK3β prolonged the half-life of cyclin D1. This was evident by the fact that, following exposure to mechanical strain, the phosphorylation level of cyclin D1 remained low in the cells. This trend was exactly inversely related to GSK3β phosphorylation. This stabilization and upregulation of cyclin D1 by PI3K-Akt pathway following mechanoactivation are paralleled by an upregulation of the cell proliferation in HDMECs, essential for angiogenesis. In addition to the Akt pathway, other pathways (e.g., MAPK) may be activated by mechanical signals to regulate cell migration during angiogenesis (55, 56).

The most striking finding of this study is the role of mechanical strain in the upregulation of HDMEC proliferation in the presence of a proinflammatory signal. Inflammation mediated by IL-1β plays a recognized role in the pathophysiology of cardiovascular disease (57). Addition of exogenous IL-1β induced G_0/G_1 phase cell-cycle arrest in cardiac microvascular endothelial cells and inhibits angiogenesis (58). In the current study, IL-1β did not induce significant VEGFR2 phosphorylation or Akt activation, and it induced only minimal GSK3β phosphorylation. Nevertheless, a significant increase in phospho-Thr286-cyclin D1 was observed in cells treated with IL-1β. The phosphorylation of cyclin D1 is associated with its increased turnover and a reduced cell proliferation, as observed in the cells treated with IL-1β. This suggests that IL-1β induces phosphorylation and subsequent degradation of

cyclin D1, independent of VEGFR2 and Akt activation, which might be achieved through activation of NF-κB pathway. In HDMECs, mechanical signals alone suppress cyclin D1 phosphorylation and subsequent degradation via GSK3β inactivation. Furthermore, in the presence of IL-1β, these signals suppress the actions of IL-1β–dependent cyclin D1 phosphorylation and degradation. Increased levels of cyclin D1 may contribute to the bypass of the cell-cycle G_1/S checkpoint to upregulate HDMEC proliferation. We also examined the antiapoptotic efficacy of DTS and found that mechanical signals also suppress the cell apoptosis induced by IL-1β. This reduction in the apoptosis by mechanical signals may provide yet another mechanism to support HDMEC survival and proliferation in a proinflammatory environment. Furthermore, to support HDMEC proliferation and angiogenesis, mechanical signals attenuate the expression of proinflammatory genes, such as *IL-1β* and *Tnf-α*, to sustain its actions in a proinflammatory environment. Interestingly, earlier studies showed that mechanical signals are anti-inflammatory signals and suppress IL-1β–induced proinflammatory gene induction via suppression of NF-κB signaling cascade (36, 37). During inflammation, strains experienced by the endothelial cells due to blood flow, edema, and tissue reorganization may be critical in maintaining proangiogenic signals in an inflammatory environment prone to tissue destruction.

Abbreviations used in this paper

|	
DTS	dynamic tensile strain
GSK3β	glycogen synthase kinase-3β
HDMEC	human dermal microvascular endothelial cell
VE	vascular endothelial
VEGF	vascular endothelial growth factor
VEGFR2	vascular endothelial growth factor receptor-2

References

1. Mammoto A, Connor KM, Mammoto T, Yung CW, Huh D, Aderman CM, Mostoslavsky G, Smith LE, Ingber DE. A mechanosensitive transcriptional mechanism that controls angiogenesis. Nature. 2009; 457:1103–1108. [PubMed: 19242469]

2. Reinhart-King CA, Fujiwara K, Berk BC. Physiologic stress-mediated signaling in the endothelium. Methods Enzymol. 2008; 443:25–44. [PubMed: 18772009]

3. Laughlin MH, Newcomer SC, Bender SB. Importance of hemodynamic forces as signals for exercise-induced changes in endothelial cell phenotype. J Appl Physiol. 2008; 104:588–600. [PubMed: 18063803]

4. Shiu YT, Weiss JA, Hoying JB, Iwamoto MN, Joung IS, Quam CT. The role of mechanical stresses in angiogenesis. Crit Rev Biomed Eng. 2005; 33:431–510. [PubMed: 16000089]

5. Helmke BP. Molecular control of cytoskeletal mechanics by hemodynamic forces. Physiology (Bethesda). 2005; 20:43–53. [PubMed: 15653839]

6. Kou B, Zhang J, Singer DR. Effects of cyclic strain on endothelial cell apoptosis and tubulogenesis are dependent on ROS production via NAD(P)H subunit p22phox. Microvasc Res. 2009; 77:125–133. [PubMed: 18801380]

7. Li M, Chiou KR, Bugayenko A, Irani K, Kass DA. Reduced wall compliance suppresses Akt-dependent apoptosis protection stimulated by pulse perfusion. Circ Res. 2005; 97:587–595. [PubMed: 16100043]

8. Liu WF, Nelson CM, Tan JL, Chen CS. Cadherins, RhoA, and Rac1 are differentially required for stretch-mediated proliferation in endothelial versus smooth muscle cells. Circ Res. 2007; 101:e44–e52. [PubMed: 17712140]

9. Orr AW, Ginsberg MH, Shattil SJ, Deckmyn H, Schwartz MA. Matrix-specific suppression of integrin activation in shear stress signaling. Mol Biol Cell. 2006; 17:4686–4697. [PubMed: 16928957]

10. Gaus K, Le Lay S, Balasubramanian N, Schwartz MA. Integrin-mediated adhesion regulates membrane order. J Cell Biol. 2006; 174:725–734. [PubMed: 16943184]

11. Ingber DE. Mechanical signaling and the cellular response to extracellular matrix in angiogenesis and cardiovascular physiology. Circ Res. 2002; 91:877–887. [PubMed: 12433832]

12. Nelson CM, Chen CS. VE-cadherin simultaneously stimulates and inhibits cell proliferation by altering cytoskeletal structure and tension. J Cell Sci. 2003; 116:3571–3581. [PubMed: 12876221]

13. Thodeti CK, Matthews B, Ravi A, Mammoto A, Ghosh K, Bracha AL, Ingber DE. TRPV4 channels mediate cyclic strain-induced endothelial cell reorientation through integrin-to-integrin signaling. Circ Res. 2009; 104:1123–1130. [PubMed: 19359599]

14. Schwartz MA, DeSimone DW. Cell adhesion receptors in mechanotransduction. Curr Opin Cell Biol. 2008; 20:551–556. [PubMed: 18583124]

15. Boyd NL, Park H, Yi H, Boo YC, Sorescu GP, Sykes M, Jo H. Chronic shear induces caveolae formation and alters ERK and Akt responses in endothelial cells. Am J Physiol Heart Circ Physiol. 2003; 285:H1113–H1122. [PubMed: 12763750]

16. Orr AW, Hahn C, Blackman BR, Schwartz MA. p21-activated kinase signaling regulates oxidant-dependent NF-kappa B activation by flow. Circ Res. 2008; 103:671–679. [PubMed: 18669917]

17. Mahabeleshwar GH, Feng W, Reddy K, Plow EF, Byzova TV. Mechanisms of integrin-vascular endothelial growth factor receptor cross-activation in angiogenesis. Circ Res. 2007; 101:570–580. [PubMed: 17641225]

18. Mammoto A, Huang S, Moore K, Oh P, Ingber DE. Role of RhoA, mDia, and ROCK in cell shape-dependent control of the Skp2-p27kip1 pathway and the G1/S transition. J Biol Chem. 2004; 279:26323–26330. [PubMed: 15096506]

19. Baker AB, Ettenson DS, Jonas M, Nugent MA, Iozzo RV, Edelman ER. Endothelial cells provide feedback control for vascular remodeling through a mechanosensitive autocrine TGF-beta signaling pathway. Circ Res. 2008; 103:289–297. [PubMed: 18583708]

20. Shibuya M. Vascular endothelial growth factor (VEGF)-Receptor2: its biological functions, major signaling pathway, and specific ligand VEGF-E. Endothelium. 2006; 13:63–69. [PubMed: 16728325]

21. Magnusson P, Rolny C, Jakobsson L, Wikner C, Wu Y, Hicklin DJ, Claesson-Welsh L. Deregulation of Flk-1/vascular endothelial growth factor receptor-2 in fibroblast growth factor receptor-1-deficient vascular stem cell development. J Cell Sci. 2004; 117:1513–1523. [PubMed: 15020678]

22. Urbich C, Stein M, Reisinger K, Kaufmann R, Dimmeler S, Gille J. Fluid shear stress-induced transcriptional activation of the vascular endothelial growth factor receptor-2 gene requires Sp1-dependent DNA binding. FEBS Lett. 2003; 535:87–93. [PubMed: 12560084]

23. Abumiya T, Sasaguri T, Taba Y, Miwa Y, Miyagi M. Shear stress induces expression of vascular endothelial growth factor receptor Flk-1/KDR through the CT-rich Sp1 binding site. Arterioscler Thromb Vasc Biol. 2002; 22:907–913. [PubMed: 12067897]

24. Zheng W, Christensen LP, Tomanek RJ. Differential effects of cyclic and static stretch on coronary microvascular endothelial cell receptors and vasculogenic/angiogenic responses. Am J Physiol Heart Circ Physiol. 2008; 295:H794–H800. [PubMed: 18586890]

25. Chang F, Lee JT, Navolanic PM, Steelman LS, Shelton JG, Blalock WL, Franklin RA, McCubrey JA. Involvement of PI3K/Akt pathway in cell cycle progression, apoptosis, and neoplastic transformation: a target for cancer chemotherapy. Leukemia. 2003; 17:590–603. [PubMed: 12646949]

26. Diehl JA, Cheng M, Roussel MF, Sherr CJ. Glycogen synthase kinase-3beta regulates cyclin D1 proteolysis and subcellular localization. Genes Dev. 1998; 12:3499–3511. [PubMed: 9832503]

27. Ryves WJ, Harwood AJ. The interaction of glycogen synthase kinase-3 (GSK-3) with the cell cycle. Prog Cell Cycle Res. 2003; 5:489–495. [PubMed: 14593744]

28. Liang J, Slingerland JM. Multiple roles of the PI3K/PKB (Akt) pathway in cell cycle progression. Cell Cycle. 2003; 2:339–345. [PubMed: 12851486]

29. Ramljak D, Calvert RJ, Wiesenfeld PW, Diwan BA, Catipovic B, Marasas WF, Victor TC, Anderson LM, Gelderblom WC. A potential mechanism for fumonisin B(1)-mediated hepatocarcinogenesis: cyclin D1 stabilization associated with activation of Akt and inhibition of GSK-3beta activity. Carcinogenesis. 2000; 21:1537–1546. [PubMed: 10910956]

30. Sawada H, Kan M, McKeehan WL. Opposite effects of monokines (interleukin-1 and tumor necrosis factor) on proliferation and heparin-binding (fibroblast) growth factor binding to human aortic endothelial and smooth muscle cells. In Vitro Cell Dev Biol. 1990; 26:213–216. [PubMed: 2312505]

31. Hébert MJ, Gullans SR, Mackenzie HS, Brady HR. Apoptosis of endothelial cells is associated with paracrine induction of adhesion molecules: evidence for an interleukin-1beta-dependent paracrine loop. Am J Pathol. 1998; 152:523–532. [PubMed: 9466579]

32. Henrich D, Seebach C, Wilhelm K, Marzi I. High dosage of simvastatin reduces TNF-alpha-induced apoptosis of endothelial progenitor cells but fails to prevent apoptosis induced by IL-1beta in vitro. J Surg Res. 2007; 142:13–19. [PubMed: 17716606]

33. Dewberry RM, King AR, Crossman DC, Francis SE. Interleukin-1 receptor antagonist (IL-1ra) modulates endothelial cell proliferation. FEBS Lett. 2008; 582:886–890. [PubMed: 18282478]

34. Chaudhuri V, Zhou L, Karasek M. Inflammatory cytokines induce the transformation of human dermal microvascular endothelial cells into myofibroblasts: a potential role in skin fibrogenesis. J Cutan Pathol. 2007; 34:146–153. [PubMed: 17244026]

35. Mullenix PS, Andersen CA, Starnes BW. Atherosclerosis as inflammation. Ann Vasc Surg. 2005; 19:130–138. [PubMed: 15714382]

36. Madhavan S, Anghelina M, Sjostrom D, Dossumbekova A, Guttridge DC, Agarwal S. Biomechanical signals suppress TAK1 activation to inhibit NF-kappaB transcriptional activation in fibrochondrocytes. J Immunol. 2007; 179:6246–6254. [PubMed: 17947700]

37. Dossumbekova A, Anghelina M, Madhavan S, He L, Quan N, Knobloch T, Agarwal S. Biomechanical signals inhibit IKK activity to attenuate NF-kappaB transcription activity in inflamed chondrocytes. Arthritis Rheum. 2007; 56:3284–3296. [PubMed: 17907174]

38. Cozzolino F, Torcia M, Aldinucci D, Ziche M, Almerigogna F, Bani D, Stern DM. Interleukin 1 is an autocrine regulator of human endothelial cell growth. Proc Natl Acad Sci USA. 1990; 87:6487–6491. [PubMed: 1697682]

39. Zhou Z, Gengaro P, Wang W, Wang XQ, Li C, Faubel S, Rivard C, Schrier RW. Role of NF-kappaB and PI 3-kinase/Akt in TNF-alpha-induced cytotoxicity in microvascular endothelial cells. Am J Physiol Renal Physiol. 2008; 295:F932–F941. [PubMed: 18632801]

40. Zachary I, Gliki G. Signaling transduction mechanisms mediating biological actions of the vascular endothelial growth factor family. Cardiovasc Res. 2001; 49:568–581. [PubMed: 11166270]

41. Singh AJ, Meyer RD, Band H, Rahimi N. The carboxyl terminus of VEGFR-2 is required for PKC-mediated down-regulation. Mol Biol Cell. 2005; 16:2106–2118. [PubMed: 15673613]

42. Shay-Salit A, Shushy M, Wolfovitz E, Yahav H, Breviario F, Dejana E, Resnick N. VEGF receptor 2 and the adherens junction as a mechanical transducer in vascular endothelial cells. Proc Natl Acad Sci USA. 2002; 99:9462–9467. [PubMed: 12080144]

43. Lin SY, Makino K, Xia W, Matin A, Wen Y, Kwong KY, Bourguignon L, Hung MC. Nuclear localization of EGF receptor and its potential new role as a transcription factor. Nat Cell Biol. 2001; 3:802–808. [PubMed: 11533659]

44. Reilly JF, Maher PA. Importin beta-mediated nuclear import of fibroblast growth factor receptor: role in cell proliferation. J Cell Biol. 2001; 152:1307–1312. [PubMed: 11257130]

45. Stachowiak MK, Maher PA, Joy A, Mordechai E, Stachowiak EK. Nuclear localization of functional FGF receptor 1 in human astrocytes suggests a novel mechanism for growth factor action. Brain Res Mol Brain Res. 1996; 38:161–165. [PubMed: 8737680]

46. Rakowicz-Szulczy ska EM, Linnenbach AJ, Koprowski H. Intracellular receptor binding and nuclear transport of nerve growth factor in intact cells and a cell-free system. Mol Carcinog. 1989; 2:47–58. [PubMed: 2543427]

47. Krolewski JJ. Cytokine and growth factor receptors in the nucleus: what's up with that? J Cell Biochem. 2005; 95:478–487. [PubMed: 15838864]

48. Tzima E, Irani-Tehrani M, Kiosses WB, Dejana E, Schultz DA, Engelhardt B, Cao G, DeLisser H, Schwartz MA. A mechanosensory complex that mediates the endothelial cell response to fluid shear stress. Nature. 2005; 437:426–431. [PubMed: 16163360]

49. Wang Y, Miao H, Li S, Chen KD, Li YS, Yuan S, Shyy JY, Chien S. Interplay between integrins and FLK-1 in shear stress-induced signaling. Am J Physiol Cell Physiol. 2002; 283:C1540–C1547. [PubMed: 12372815]

50. Liu Y, Sweet DT, Irani-Tehrani M, Maeda N, Tzima E. Shc coordinates signals from intercellular junctions and integrins to regulate flow-induced inflammation. J Cell Biol. 2008; 182:185–196. [PubMed: 18606845]

51. Lampugnani MG, Orsenigo F, Gagliani MC, Tacchetti C, Dejana E. Vascular endothelial cadherin controls VEGFR-2 internalization and signaling from intracellular compartments. J Cell Biol. 2006; 174:593–604. [PubMed: 16893970]

52. Dormond O, Madsen JC, Briscoe DM. The effects of mTOR-Akt interactions on anti-apoptotic signaling in vascular endothelial cells. J Biol Chem. 2007; 282:23679–23686. [PubMed: 17553806]

53. Masuyama N, Oishi K, Mori Y, Ueno T, Takahama Y, Gotoh Y. Akt inhibits the orphan nuclear receptor Nur77 and T-cell apoptosis. J Biol Chem. 2001; 276:32799–32805. [PubMed: 11438550]

54. Rosner M, Hanneder M, Freilinger A, Hengstschläger M. Nuclear/cytoplasmic localization of Akt activity in the cell cycle. Amino Acids. 2007; 32:341–345. [PubMed: 17357828]

55. Kadohama T, Akasaka N, Nishimura K, Hoshino Y, Sasajima T, Sumpio BE. p38 Mitogen-activated protein kinase activation in endothelial cell is implicated in cell alignment and elongation induced by fluid shear stress. Endothelium. 2006; 13:43–50. [PubMed: 16885066]

56. Huang C, Jacobson K, Schaller MD. MAP kinases and cell migration. J Cell Sci. 2004; 117:4619–4628. [PubMed: 15371522]

57. Ukimura A, Terasaki F, Fujioka S, Deguchi H, Kitaura Y, Isomura T, Suma H. Quantitative analysis of cytokine mRNA expression in hearts from patients with nonischemic dilated cardiomyopathy (DCM). J Card Surg. 2003; 18(Suppl 2):S101–S108. [PubMed: 12930277]

58. Mountain DJ, Singh M, Singh K. Interleukin-1beta-mediated inhibition of the processes of angiogenesis in cardiac microvascular endothelial cells. Life Sci. 2008; 82:1224–1230. [PubMed: 18501931]
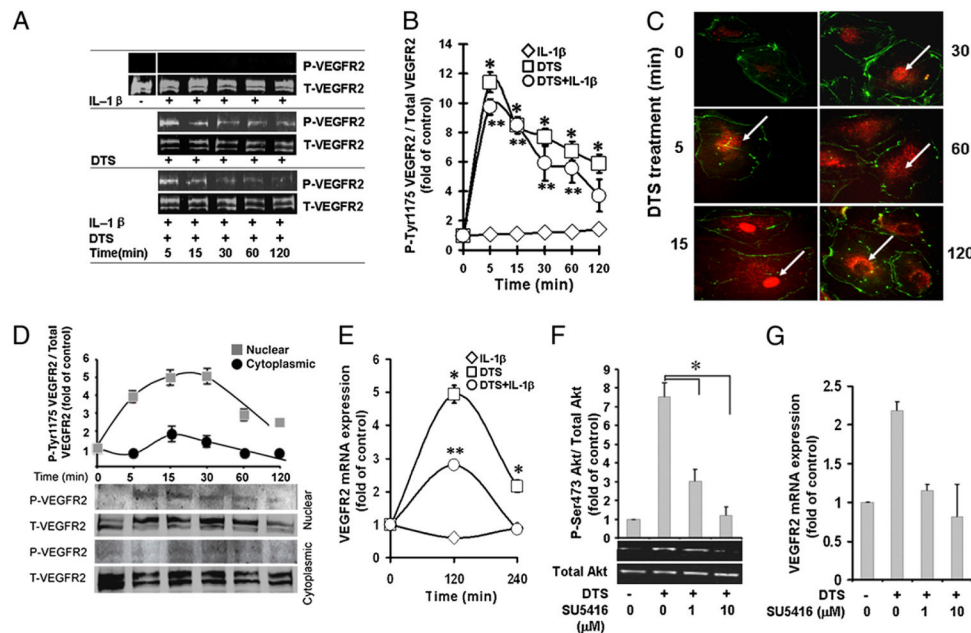
FIGURE 1.
Mechanical strain upregulates VEGFR2 activation. HDMECs were treated alone with DTS, IL-1β, or DTS and IL-1β together for various lengths of time. Subsequently, cells were analyzed for VEGFR2 Tyr1175 phosphorylation analyzed by Western blot analysis (*A*); the relative phospho-Tyr1175-VEGFR2 assessed by digitization of phosphorylated bands shown in *A* (*B*); relative presence of phospho-VGEFR2 in the cytoplasm and nucleus, as indicated by arrows, by immunofluorescence using phospho-Tyr1175-VEGFR2–specific Ab (*C*) (original magnification ×400); Western blot analysis of nuclear and cytoplasmic extracts of HDMECs showing localization of phospho-VEGFR2 in the nucleus after mechanoactivation (*D*); time course of VEGFR2 mRNA expression by real-time PCR (*E*); inhibition of Ser473-Akt phosphorylation by VEGFR2 antagonist SU5416 (*F*); and VEGFR2 mRNA expression in the presence of SU5416 (*G*). All experiments were performed in triplicate and repeated three times (*A–C, E, F*) or two times (*D, G*). *$p < 0.05$, cells treated with DTS versus untreated control group or inhibitor-treated group; **$p < 0.05$, cells treated with IL-1β and DTS compared with IL-1β.
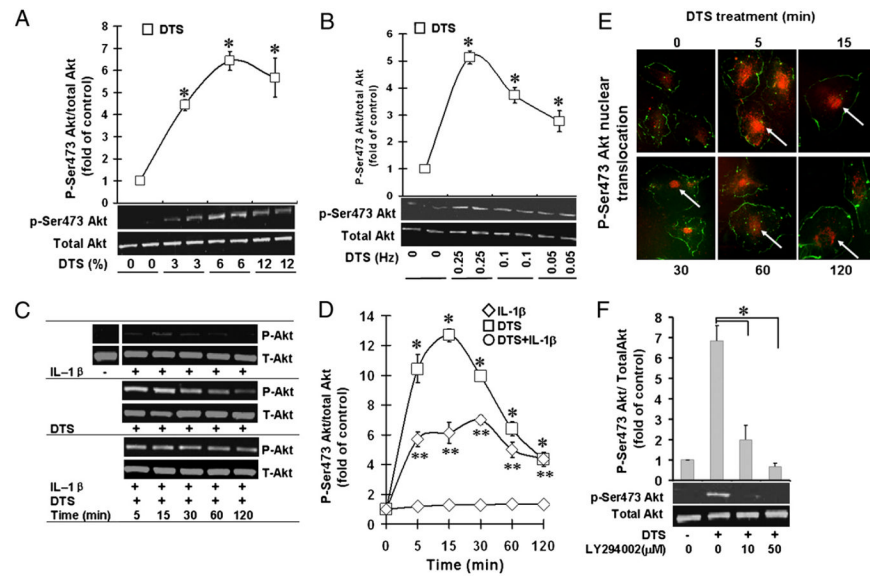
FIGURE 2.

Mechanicalstrain upregulatesAkt activation. HDMECs were exposed to DTS, IL-1β, or DTS and IL-1β to assess the Akt phosphorylation by Western blot analysis at various magnitudes of DTS at 0.25 Hz (*A*); at various frequencies of DTS at a magnitude of 6% (*B*); during various time intervals at a magnitude of 6% and 0.25 Hz (*C*) and relative phosphorylation of Ser473 by digitization of phosphorylated bands (*D*). *E*, Analysis of phospho-Ser473-Akt by immunofluorescence showing its cytoplasmic and nuclear translocation, indicated by arrows, between 5 and 120 min of DTS exposure (original magnification ×400). *F*, Western blot analysis showing Ser473-Akt phosphorylation in the presence of PI3K inhibitor LY294002. All experiments were performed in triplicates and repeated three times. *p <0.05, cells treated with DTS versus untreated control group or inhibitor-treated group; **p <0.05, cells treated with IL-1β and DTS compared with IL-1β alone.
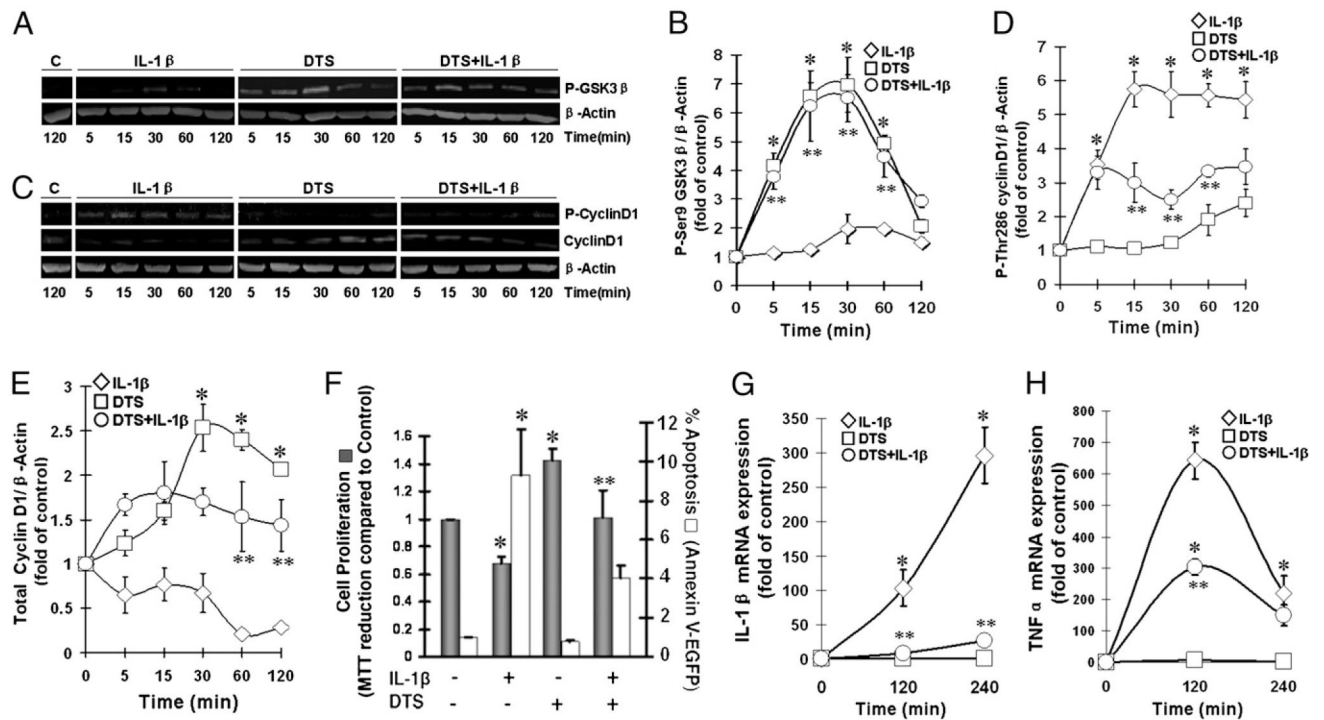
FIGURE 3.
Mechanical signals upregulate HDMECs proliferation by inhibiting GSK3β-dependent phosphorylation of cyclin D1. HDMECs were subjected to DTS in the presence or absence of IL-1β and analyzed by Western blot analysis to assess phosphorylation of Ser9-GSK3β from 5–120 min (*A*); the relative phosphorylation of GSK3β by digitization of fluorescence in each band (*B*); phospho-Thr286 cyclin D1 and total cyclin D1 from 5–120 min (*C*); and the relative levels of phosphorylated cyclin D1 (*D*) and total cyclin D1 (*E*), by digitization of fluorescence in each band. *F*, DTS induces cell proliferation and suppresses IL-1β–induced apoptosis in HDMECs. Cells were subjected to DTS in the presence or absence of IL-1β for 60 min/day for 2 d; on day 3, cell proliferation was assessed by MTT assay (solid bars) and cell apoptosis was assessed by Annexin V-EGFP (open bars). Expression of IL-1β (*G*) and TNF-α (*H*) mRNA in HDMECs subjected to DTS in the presence or absence of IL-1β for 2 or 4 h. All experiments were performed in triplicates and repeated three times. *$p < 0.05$, cells treated with DTS or IL-1β alone versus untreated control group; **$p < 0.05$, cells treated with IL-1β and DTS compared with IL-1β alone.